Journal of Radiation Research and Applied Sciences 18 (2025) 101690

Contents lists available at ScienceDirect

Journal of Radiation Research and Applied Sciences

journal homepage: www.journals.elsevier.com/journal-of-radiation-research-and-applied-sciences

Regular perturbation characterization of transient MHD dissipation penetrable flow with thermal radiative flux

Syed M. Hussain [a], Hina Zahir [b,*], Muhamamd Taskeen Raza [c], Bandar M. Fadhl [d], Mohamed R. Eid [e], Wasim Jamshed [f,g,h,1], Siti Suzilliana Putri Mohamed Isa [i,j], Kamel Guedri [d]

[a] Department of Mathematics, Faculty of Science, Islamic University of Madinah, Madinah, 42351, Saudi Arabia
[b] Department of Mathematics, Benazir Bhutto Shaheed University (BBSU), Peshawar, 25000, Pakistan
[c] Department of Electrical Engineering, Lahore College for Women University, Lahore, Pakistan
[d] Mechanical Engineering Department, College of Engineering and Architecture, Umm Al-Qura University, P. O. Box 5555, Makkah, 21955, Saudi Arabia
[e] Center for Scientific Research and Entrepreneurship, Northern Border University, Arar, 73213, Saudi Arabia
[f] Department of Mathematics, Capital University of Science and Technology (CUST), Islamabad, 44000, Pakistan
[g] College of Engineering, Al-Ayen Iraqi University, An Nasiriyah, 64001, Iraq
[h] Department of Computer Engineering, Biruni University, Topkapi, Istanbul, Turkey
[i] Centre for Foundation Studies in Science of Universiti Putra Malaysia, Universiti Putra Malaysia, UPM Serdang, 43400, Selangor, Malaysia
[j] Institute for Mathematical Research, Universiti Putra Malaysia, UPM Serdang, 43400, Selangor, Malaysia

ARTICLE INFO

Keywords:
Unsteady convection
MHD
Dissipation
Porous media
Thermal radiation
Perturbation technique

ABSTRACT

This study investigates the transient magnetohydrodynamic (MHD) flow and heat and mass transfer over an inclined, radiative, and permeable surface under the influence of viscous dissipation and Ohmic heating in a porous medium. A regular perturbation technique is employed to solve the governing coupled, nonlinear partial differential equations that describe the velocity, temperature, and concentration fields. The analysis focuses on key physical parameters, including the skin friction coefficient, Nusselt number, and Sherwood number, along with the corresponding field profiles. The results highlight the significant impact of inclination angle, porosity, and thermal radiation on the transport behavior. Specifically, thermal radiation is found to reduce both the temperature distribution and the Nusselt number, indicating a damping effect on thermal transport. Conversely, the presence of a heat source elevates the temperature while enhancing heat transfer. Additionally, the Soret number contributes to an increase in both temperature and solute concentration due to thermal diffusion effects. The findings correspond well with previously published studies. In other words, when the inclined angle, porous parameter, and radiation parameter are not considered, all outcomes closely resemble those of the previously published works. This study offers valuable insights applicable to various industrial processes, including chemical manufacturing and thermal management systems.

1. Introduction

Natural convection is utilized in various applications, including chemical catalytic reactors, electronic cooling equipment, nuclear reactor cooling, solar power collectors, and thermal and insulating engineering. Unsteady Magnetohydrodynamic (MHD) flows are essential because they are associated with fluid transients, such as those found in forging, MHD energy producers, MHD accelerators, and controlled thermonuclear reactors. Considering the relevance of such studies, several researchers have studied unsteady hydromagnetic convective flow through liquid-saturated porous media. MHD describes the interplay between magnetic fields and electrical conductance fields. In MHD flows, the existence of a magnetized force causes electric currents to be induced inside the fluid. This leads to the formation of a Lorentz force, which, in turn, alters the fluid flow behavior over time. The interaction between these two factors is crucial for enhancing operations across various sectors. Recent developments in quantum mechanics (MHD) research have centered on the creation of computational tools and experimental methodologies to analyze the intricate dynamics of MHD systems. There are numerous applications for MHD, including the

* Corresponding author. PhD Mathematics
E-mail address: moudah1@yahoo.com (H. Zahir).
[1] (Gold Medalist).

https://doi.org/10.1016/j.jrras.2025.101690
Received 9 May 2025; Received in revised form 1 June 2025; Accepted 5 June 2025
Available online 16 June 2025
1687-8507/

generation of electricity, material processing, and space exploration. For instance, maximum heat density (MHD) generators in power plants are responsible for converting thermal energy into electricity. In the materials treatment industry, MHD pumping and mixers are used to regulate the behaviour of fluids. Additionally, MHD turbines play a worthy role in the motion control of satellites for the purpose of space exploration. Chemical reaction mass transfer effects in food processing, agricultural fields, and cooling towers. Sandeep and Sugunamma (Sandeep and Sugunamma, 2013) studied the magneto-fluid flow via a porous vertical surface with the consequence of a chemical reaction. Ibrahim and Makinde (Ibrahim et al., 2010) explored chemically reacting MHD flow with suction on a moving vertical surface. Time-dependent chemically reacting hydromagnetic liquid flows across a vertical surface with continuous flux (Makinde, 2012). Zhou et al. (Zhou et al., 2024) reported the thermosolutal MHD fluid flow with heat source effect. Recently, the MHD convection in various types of fluids has been published, including Carreau fluid (Isa et al., 2024) and Casson fluid (Kumar et al., 2023), among others.

Alterations in temperature are the root cause of the concentration gradient, which in turn is the root cause of the Soret process. Temperature changes are a consequence of mass concentration, which results in an energy flow that is described as the Dufour impact. Both the Soret and Dufour effects cannot be reversed after they have been applied. This irreversible phenomenon is used in a wide variety of applications within the field of chemical engineering. It has been shown via published works that the Soret and Dufour effects have several applications within the realm of fluid dynamics. Below the influences of Dufour and Soret, variances in density are the driving force behind fluids. Variability in density is because of variation in temperatures in addition to differences in mass concentration. In isotope mixture and gas separation, the Soret effect is applied. The Soret effect focuses on mass transfer, driving tiny particles from heat to cold surfaces. This phenomenon helps remove small particles from gas streams and investigates particle deposition on turbine blades. Mass transfer affects all separation processes in chemical engineering, including drying, distillation, extraction, and absorption. Therefore, the relevant studies regarding the Soret impact acting on the fluid flow with additional impacts such as thermophoresis (Rahman et al., 2012), thermal radiation (Alam et al., 2008), and heat source (Karraiah et al., 2013).

The term "thermal radiation" describes the process of heat transmission that occurs by electromagnetic radiation, most often in the infrared region. When it comes to high-temperature situations, where radiant heat transmission might take precedence over conductive or convective heat transfer, this impact is very important to consider. A substantial amount of attention has been put into recent research on the comprehension of thermal convective fluxes, as well as the function that thermal radiation plays in a variety of technical and manufacturing operations. For the purpose of managing system temperatures and heat transfer rates, thermal radiation is of utmost significance. Its applications range from the advancement of technological devices to the provision of healthcare. The interaction between peristaltic motion and heat radiation has not been investigated by a large number of scholars, despite the relevance of this topic. Thermal radiation plays a key function in gas turbines, car engines, high-temperature heat exchangers, and combustion chambers, which operate at high temperatures. The heat transfer properties of natural convection boundary layer flow rely on thermal boundary conditions. Cess (Cess, 1966) used Rosseland diffusion approximation to explore radiating convective boundary layers with buoyancy effects. Makinde and Olanrewaju (Makinde et al., 2010) examined how a convective thermal boundary layer affects buoyancy force in the radiating fluid model. Meanwhile, Makinde (Makinde, 2005) explored radiating convective flows in the heat-mass transfer fluid system. Nandkeolyar et al. (Nandkeolyar et al., 2013) explored transient magnetic convective dusty fluid flow via a moving vertical surface with ramping temperature. Dharmaiah et al. (Dharmaiah et al., 2022) examined the influences of thermal radiation in the non-Newtonian liquid model.

Heat-mass transfer in liquids across porous media has garnered a lot of interest since this research has extensive applications in biological sciences and medicine. These include biofluid movement in blood vascular tissue and moisture flow through porous industrial materials. Hence, the fluid flow model via porous materials has been reported, because of the influences of suction (Das et al., 2006), heat source (Das et al., 2010), oscillatory state (Makinde et al., 2005), and MHD flow (Eid et al., 2017). Electrical cooling, solar energy classifications, burning systems, materials processing, and microscale heat are some of the applications in engineering that may benefit from the emergence of thermal radiative with viscous dissipative fluxes. It is possible to ascertain the variation in temperature and the rates of heat transmission by utilizing the combinations of thermal radiative (which is caused by the emission of electromagnetic radiation because of temperature disparities) and viscous dissipative fluxes (which take place caused by internal resistance).

Viscous dissipative flux is significant in geophysical flows, instrumentation, tribology, lubrication, polymer manufacture, and engineering processes. In fluid mechanics, viscous forces reduce variable velocity gradients. Viscous dissipation is the irreversible conversion of shear fluid-induced work on consecutive layers into heat. This largely irreversible mechanism converts kinetic energy into internal fluid energy. The main parameter that expresses the impact of viscous dissipative fluxing is the Eckert number (*Ec*). Gebhart (Gebhart, 1962) showed the relevance of heat-dissipative convective flow down a semi-vertical isothermal surface. Ganesan et al. (Ganesan et al., 2013) studied Ohmic heating in double-stratified convected flow with radiation. Rashidi and the effect of dissipative Ohmic heating in a steady MHD fluid convection over a spinning disk (Rashidi et al., 2012) and inclined surface (Alam et al., 2009) have been reported. Osalusi et al. (Osalusi et al., 2007) analyzed dissipative Ohmic heating impacts on steady heat transfer with Hall and ion-slip currents. Chien-Hsin (Chien-Hsin, 2004) integrated MHD-free convected dissipative Ohmic heating impacts. The dissipative impacts towards a fluid flow via an oblique surface have been reported, subjected to the projected magnetic field (Dharmaiah et al., 2019) and thermophoresis factor (Dharmaiah et al., 2020). This research uses a fundamental framework to carry out chemical processes. The aim of this examination is to explore how variations in the concentration of substances influence the flow and heat transference in multilayer systems. The kinetics of the reaction are modelled on the assumption of a first-order reaction, which is a model that is frequently applicable in situations where only one reactant eventually decays into products. Through the use of this presumption, the mathematical modelling is simplified while yet preserving the fundamental dynamics of the reaction process. In future studies, researchers might explore more complicated reactions, like those involving multiple steps or different substances, and give specific examples to make the research more relevant and thorough. Radiation and chemical processes may overlap in some situations. Radioactivity, for example, can initiate or quicken chemically reactive processes. This effect is readily apparent in operations such as radiolysis, wherein ionising radiative flux is used to break chemical bonds, resulting in the formation of new particle species. Applications include both radiation-induced polymerisation in the manufacturing of certain substances and radiative-supported chemical synthesis in labs. A comprehension of the interaction between radiative flux and chemically reactive processes, as well as the ability to manipulate such interactions, has practical ramifications in the fields of nuclear chemistry and chemical industrial operations. The assumptions about the reactions and chemicals involved are logical because they are important for real-world applications, easy to test, and consistent with past research. 1st-order reaction kinetics are extensively employed in research similar to fluid dynamics because they are simple and can show the basic effects that chemically reactive processes have on flow and heat transmission. This hypothesis is reflective of the common circumstances that exist in real-world routines, such as microfluidics and polymeric manufacturing, where reactive rates are mostly reliant on concentration.

The novelty of this research lies in the analytical investigation of unsteady magnetohydrodynamic (MHD) flow and coupled heat–mass transfer over an inclined, radiative, and permeable plate, incorporating the combined effects of viscous dissipation, Ohmic heating (Ananda Reddy et al., 2009), thermal radiation, and the Soret effect. Unlike previous studies that often neglect the simultaneous influence of these parameters, this work provides a comprehensive regular perturbation solution to a highly coupled, nonlinear system (Eswaramoorthi et al., 2025; Eswaramoorthi & Sivasankaran, 2022; Mallawi et al., 2022; Reddy et al., 2023; Sindhu et al., 2023; Srinivasa et al., 2024). The study introduces a unique geometric and physical configuration penetrable flow on a slanted radiative surface under transient conditions which has not been thoroughly explored in existing literature. The results offer new insights into controlling thermal and concentration boundary layers in porous and radiative environments, with practical implications for energy systems, chemical processing, and heat management technologies.

Motivated by the factors mentioned above and contributions, this work investigates the influences of regulatory factors, like viscous dissipation, thermal radiative flux, and the Soret parameter, in the fluid flow system with the presence of chemically reactive processes. On an inclined, radiative, permeable plate, the purpose of this examination is to explore the behaviour of fluid flow and heat and mass transmission under unstable circumstances brought about by viscous dissipative flux and Ohmic heating in porous medium. Through the use of a perturbation technique, we have attempted to analyze the combined non-linear PDEs that regulate the system. The results are determined by a multitude of distinct characteristics, including physical parameters (like the skin frictional factor, the Nusselt numbers, and the Sherwood numbers) and profiles (including velocity, temperature, and concentrations).

The main objective of this study is to analyze transient MHD flow and coupled heat–mass transfer over an inclined, radiative, permeable plate considering viscous dissipation, Ohmic heating, and the Soret effect in porous material. Using a regular perturbation technique, the study provides insights applicable to optimizing thermal systems in chemical processing, energy transport, and porous media engineering. Recent advancements cited in references (Prasad et al., 2023; Rajakumar et al., 2020b, 2024a, 2024b, 2025) highlight current developments in the field.

2. Mathematical formulation

- The flow is assumed to be laminar, incompressible, and electrically conducting.
- The porous medium is considered homogeneous and isotropic with constant porosity and permeability.
- The magnetic Reynolds number is very small, so the induced magnetic field is neglected compared to the applied magnetic fields.
- Thermal radiation is modelled using the Rosseland approximation, valid for optically thick media.
- Effects of viscous dissipation and Ohmic heating are included.
- Chemical reactions are assumed to be homogeneous and of first-order.
- The boundary layer approximations are applied, restricting analysis near the plate.
- Effects such as turbulence, compressibility, variable fluid properties, and non-Newtonian behavior are neglected.
- The regular perturbation method assumes small and smooth variations in flow parameters.

The fluid flow model via an oblique porous surface is considered, including thermal radiative fluxing, viscous dissipation, chemical reaction, and Soret effects. The model is presented by using Cartesian coordinates, where the plate is projected from the reference horizontal vector ($x-$ axis) (Fig. 1). The regulating formulas (Ananda Reddy et al., 2009; Dharmaiah et al., 2020) are presented as continuity (Eq. (1)), momentum (Eq. (2)), energy (Eq. (3)), and diffusion (Eq. (4)):

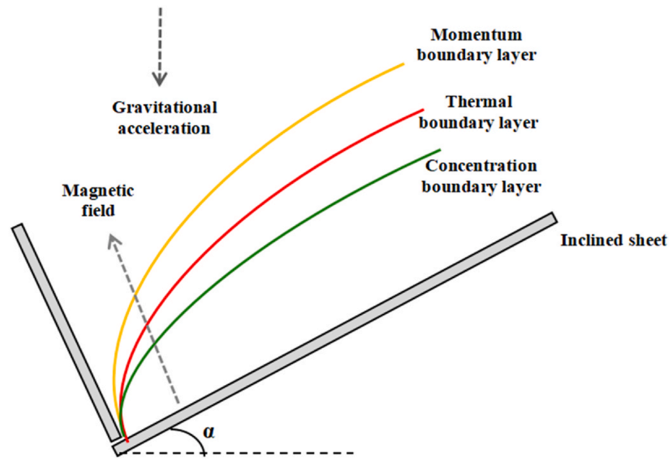

Fig. 1. The problem's geometry.

$$\frac{\partial v^*}{\partial y^*} = 0 \Rightarrow v^* = -v_0 (v_0 > 0) \tag{1}$$

$$\frac{\partial u^*}{\partial t^*} + v^* \frac{\partial u^*}{\partial y^*} = \upsilon \frac{\partial^2 u^*}{\partial y^{*\,2}} + g\beta \cos\alpha (T^* - T_\infty) + g\beta^* \cos\alpha (C^* - C_\infty) - \frac{\sigma B_0^2}{\rho} u^* - \frac{\upsilon}{K^*} u^* \tag{2}$$

$$\frac{\partial T^*}{\partial t^*} + v^* \frac{\partial T^*}{\partial y^*} = \frac{k}{\rho C_p} \frac{\partial^2 T^*}{\partial y^{*\,2}} + \frac{Q_h}{\rho C_p} (T^* - T_\infty) + \frac{\upsilon}{C_p} \left(\frac{\partial u^*}{\partial y^*} \right)^2 + \frac{\sigma B_0^2}{\rho C_p} u^{*\,2} + \frac{\upsilon}{C_p K^*} u^{*\,2} - \frac{1}{\rho C_p} \frac{\partial q^*}{\partial y^*} \tag{3}$$

$$\frac{\partial C^*}{\partial t^*} + v^* \frac{\partial C^*}{\partial y^*} = D \frac{\partial^2 C^*}{\partial y^{*\,2}} - K_1 (C^* - C_\infty) + D_1 \frac{\partial^2 T^*}{\partial y^{*\,2}} \tag{4}$$

These are the appropriate boundary constraints (Ananda Reddy et al., 2009; Dharmaiah et al., 2020):

$$u^* = 0, T^* = T_w, C^* = C_w \; at \; y^* = 0 \tag{5}$$

$$u^* \to 0, T^* \to T_\infty, C^* \to C_\infty \; as \; y^* \to \infty \tag{6}$$

On the right-side of Eq. (2), the 2nd and 3rd terms are called inclined convective, the 4th term is called magnetic, and the 5th term is called the porous effect. On the right-side of Eq. (3), 2nd term is heat generation, 3rd term is viscous dissipative flux, 4th term is the Ohmic heating effect, and the last one is the radiation effect. In addition, on the right-side of Eq. (4), 2nd term is a chemical reaction, 3rd term is thermal diffusion. Non-dimensional quantities are:

$$F = \frac{16 \tilde{a} \sigma^* \upsilon^2 T_\infty^{*3}}{k v_0^2}, Q = \frac{Q_h \upsilon}{\rho C_p v_0^2}, Kr = \frac{\upsilon k_1}{v_0^2}, S_0 = \frac{D_1 (T_w - T_\infty)}{\upsilon (C_w - C_\infty)}, M^2 = \frac{\sigma B_0^2 \upsilon}{\rho v_0^2}; \quad Ec = \frac{v_0^2}{C_p (T_w - T_\infty)}, Pr = \frac{\upsilon \rho C_p}{k}, K^* = \frac{k \upsilon^2}{v_0^2}; \tag{7}$$

Spatial radiant absorption for gray gas with a light optical layer is:

$$\frac{\partial q_r}{\partial y^*} = -4 \tilde{a} \sigma^* \left(T_\infty^{*\,4} - T^{*4} \right) \tag{8}$$

Substituting eq. (7) in (2)–(4) with (5)–(6), yields to:

$$\frac{\partial u}{\partial t}-\frac{\partial u}{\partial y}=\frac{\partial^2 u}{\partial y^2}+a\theta+b\varphi-N_4u \tag{9}$$

$$\frac{\partial\theta}{\partial t}-\frac{\partial\theta}{\partial y}=\frac{1}{Pr}\frac{\partial^2\theta}{\partial y^2}+Q\theta+Ec\left(\frac{\partial u}{\partial y}\right)^2+EcN_3u^2-\frac{F}{Pr}\theta \tag{10}$$

$$\frac{\partial\phi}{\partial t}-\frac{\partial\phi}{\partial y}=\frac{1}{Sc}\frac{\partial^2\phi}{\partial y^2}-Kr\phi-N_4u+S_0\frac{\partial^2\theta}{\partial y^2} \tag{11}$$

with BCs:

$$y=0:u=0,\theta=1,\phi=1 \tag{12}$$

$$y\to\infty:u\to0,\theta\to0,\phi\to0 \tag{13}$$

Where $N_3=\frac{1}{K}$, $N_4=M^2+\frac{1}{K}$, $a=Gr\cos\alpha$, $b=Gm\cos\alpha$.

3. The solution to the problem

Assumed solution of the problem as:

$$u(y,t)=f_0+Ecf_1+O\left(Ec^2\right) \tag{14}$$

$$\theta(y,t)=g_0+Ecg_1+O\left(Ec^2\right) \tag{15}$$

$$\phi(y,t)=h_0+Ech_1+O\left(Ec^2\right) \tag{16}$$

Substituting equations (15)–(17) in Eqs. (10)–(12) with Eqs. (13) and (14), and power equivalence Ec, the following was obtained:

0^{th} order equations:

$$\left.\begin{aligned}&\frac{\partial f_0}{\partial t}-\frac{\partial f_0}{\partial y}=\frac{\partial^2 f_0}{\partial y^2}+ag_0+bh_0-N_4f_0,\\&Pr\left(\frac{\partial g_0}{\partial t}-\frac{\partial g_0}{\partial y}\right)=\frac{\partial^2 g_0}{\partial y^2}+(Pr\,Q-F)g_0,\\&Sc\left(\frac{\partial h_0}{\partial t}-\frac{\partial h_0}{\partial y}\right)=\frac{\partial^2 h_0}{\partial y^2}-ScKrh_0+ScS_0\frac{\partial^2 g_0}{\partial y^2}.\end{aligned}\right\} \tag{17}$$

First-order equations:

$$\left.\begin{aligned}&\frac{\partial f_1}{\partial t}-\frac{\partial f_1}{\partial y}=\frac{\partial^2 f_1}{\partial y^2}+ag_1+bh_1-N_4f_1,\\&Pr\left(\frac{\partial g_1}{\partial t}-\frac{\partial g_1}{\partial y}\right)=\frac{\partial^2 g_1}{\partial y^2}+Pr\left(\frac{\partial f_0}{\partial y}\right)^2+Pr\,N_3f_0^2+(Pr\,Q-F)g_1,\\&Sc\left(\frac{\partial h_1}{\partial t}-\frac{\partial h_1}{\partial y}\right)=\frac{\partial^2 h_1}{\partial y^2}-ScKrh_1+ScS_0\frac{\partial^2 g_1}{\partial y^2}.\end{aligned}\right\} \tag{18}$$

The corresponding BCs are:

$$\left.\begin{aligned}&y=0:f_0=0,f_1=0,g_0=1,g_1=0,h_0=1,h_1=0,\\&y\to\infty:f_0\to0,f_1\to0,g_0\to0,g_1\to0,h_0\to0,h_1\to0\end{aligned}\right\} \tag{19}$$

To reduce PDEs, are:

$$\left.\begin{aligned}&f_0(y,t)=f_{00}+f_{01}e^{nt},\\&f_1(y,t)=f_{10}+f_{11}e^{nt},\\&g_0(y,t)=g_{00}+g_{01}e^{nt},\\&g_1(y,t)=g_{10}+g_{11}e^{nt},\\&h_0(y,t)=h_{00}+h_{01}e^{nt},\\&h_1(y,t)=h_{10}+h_{11}e^{nt},\end{aligned}\right\} \tag{20}$$

Substituting (20) into (17)–(18) and equating harmonic and nonharmonic terms, leads to:

$$\left.\begin{aligned}&f''_{00}+f'_{00}-N_4f_{00}=-ag_{00}-bh_{00},\\&f''_{01}+f'_{01}-(N_4+n)f_{01}=-ag_{01}-bh_{01},\\&f''_{10}+f'_{10}-N_4f_{10}=-ag_{10}-bh_{10},\\&f''_{11}+f'_{11}-(N_4+n)f_{11}=-ag_{11}-bh_{11},\\&g''_{00}+Pr\,g'_{00}+(Pr\,Q-F)g_{00}=0,\\&g''_{01}+Pr\,g'_{01}+(Pr\,Q-F-nPr)g_{01}=0,\\&g''_{10}+Pr\,g'_{10}+(Pr\,Q-F)g_{10}=-Pr\,f'^{\,2}_{00}-Pr\,N_3f_{00}^2,\\&g''_{11}+Pr\,g'_{11}+(Pr\,Q-F-nPr)g_{11}=-2\,Pr\,f'_{00}f'_{00}-2\,Pr\,N_3f_{00}^2f_{01},\\&h''_{00}+Sch'_{00}-ScKrh_{00}=-ScS_0g''_{00},\\&h''_{01}+Sch'_{01}-Sc(Kr+n)h_{01}=-ScS_0g''_{01},\\&h''_{10}+Sch'_{10}-ScKrh_{10}=-ScS_0g''_{10},\\&h''_{11}+Sch'_{11}-Sc(Kr+n)h_{11}=-ScS_0g''_{11}.\end{aligned}\right\} \tag{21}$$

The corresponding BCs are:

$$\left.\begin{aligned}&at\ y=0:\\&f_{00}=0,f_{01}=0,f_{10}=0,f_{11}=0,\\&g_{00}=1,g_{01}=0,g_{10}=0,g_{11}=0,\\&h_{00}=1,h_{01}=0,h_{10}=0,h_{11}=0,\\&as\ y\to\infty:\\&f_{00}\to0,f_{01}\to0,f_{10}\to0,f_{11}\to0,\\&g_{00}\to0,g_{01}\to0,g_{10}\to0,g_{11}\to0,\\&h_{00}\to0,h_{01}\to0,h_{10}\to0,h_{11}\to0.\end{aligned}\right\} \tag{22}$$

The solutions of (21) applying boundary conditions (22) are:

$$f_{00}=E_5e^{-a_5y}+E_3e^{-a_1y}-E_4e^{-a_3y} \tag{23}$$

$$\begin{aligned}f_{10}=&E_{38}e^{-a_{11}y}-E_{27}e^{-a_9y}+E_{28}e^{-a_7y}+E_{29}e^{-2a_3y}+E_{30}e^{-2a_5y}+E_{31}e^{-2a_1y}\\&+E_{32}e^{-(a_5+a_3)y}+E_{33}e^{-(a_5+a_1)y}+E_{34}e^{-(a_1+a_3)y}\end{aligned} \tag{24}$$

$$f_{01}=f_{11}=0 \tag{25}$$

$$g_{00}=e^{-a_1y} \tag{26}$$

$$\begin{aligned}g_{10}=&E_{15}e^{-a_7y}-E_6e^{-2a_3y}-E_7e^{-2a_5y}-E_8e^{-2a_1y}+E_9e^{-(a_5+a_3)y}-E_{10}e^{-(a_5+a_1)y}\\&+E_{11}e^{-(a_1+a_3)y}\end{aligned} \tag{27}$$

$$g_{01}=g_{11}=0 \tag{28}$$

$$h_{00}=E_2e^{-a_3y}-E_1e^{-a_1y} \tag{29}$$

$$\begin{aligned}h_{10}=&E_{26}e^{-a_9y}-E_{16}e^{-a_7y}+E_{17}e^{-2a_3y}+E_{18}e^{-2a_5y}+E_{19}e^{-2a_1y}-E_{20}e^{-(a_5+a_3)y}\\&+E_{21}e^{-(a_5+a_1)y}-E_{22}e^{-(a_1+a_3)y}\end{aligned} \tag{30}$$

$$h_{01} = h_{11} = 0. \tag{31}$$

The solutions of the liquid flow are:

$$u(y,t) = \left(E_5 e^{-a_5 y} + E_3 e^{-a_1 y} - E_4 e^{-a_3 y}\right) + Ec\big(E_{38} e^{-a_{11} y} - E_{27} e^{-a_9 y} + E_{28} e^{-a_7 y} + E_{29} e^{-2a_3 y} + E_{30} e^{-2a_5 y} + E_{31} e^{-2a_1 y} + E_{32} e^{-(a_5+a_3)y} + E_{33} e^{-(a_5+a_1)y} + E_{34} e^{-(a_1+a_3)y}\big) \tag{32}$$

$$\theta(y,t) = \left(e^{-a_1 y}\right) + Ec\big(E_{15} e^{-a_7 y} - E_6 e^{-2a_3 y} - E_7 e^{-2a_5 y} - E_8 e^{-2a_1 y} + E_9 e^{-(a_5+a_3)y} - E_{10} e^{-(a_5+a_1)y} + E_{11} e^{-(a_1+a_3)y}\big) \tag{33}$$

$$\varphi(y,t) = \left(E_2 e^{-a_3 y} - E_1 e^{-a_1 y}\right) + Ec\big(E_{26} e^{-a_9 y} - E_{16} e^{-a_7 y} + E_{17} e^{-2a_3 y} + E_{18} e^{-2a_5 y} + E_{19} e^{-2a_1 y} - E_{20} e^{-(a_5+a_3)y} + E_{21} e^{-(a_5+a_1)y} - E_{22} e^{-(a_1+a_3)y}\big) \tag{34}$$

$$\left.\begin{aligned} C_f &= \frac{\tau_{xy}}{v_0^2} = \left(\frac{\partial u}{\partial y}\right)_{y=0}, \\ Nu &= -x\frac{\left(\frac{\partial \theta}{\partial y}\right)_{y=0}}{(T_w - T_\infty)} \Rightarrow \frac{Nu_x}{Re_x} = -\left(\frac{\partial \theta}{\partial y}\right)_{y=0}, \\ h &= -x\frac{\left(\frac{\partial \varphi}{\partial y}\right)_{y=0}}{(C_w - C_\infty)} \Rightarrow \frac{Sh_x}{Re_x} = -\left(\frac{\partial \varphi}{\partial y}\right)_{y=0}. \end{aligned}\right\} \tag{35}$$

4. Results and discussion

The presence of viscous dissipative flux and Ohmic heating in the transverse MHD fluid flow and heat and mass transmission have been analyzed, influenced by thermal radiation, thermo-diffusion, and chemical reactions. The numerical solutions obtained from this study are presented for the physical factors (surface frictional factor, Nusselt numbers, and Sherwood numbers) and profiles (velocity, temperature, and concentrations). The authors' opinion goes to do numerical simulations for two scenarios: Scenario I, where $(Gr, Gm) < 0$ (flow on a heated surface), and Scenario II, when $(Gr, Gm) > 0$ (flow on a cooled surface). In this paper, Scenario I is indicated by these values: $Gr = -2$ and $Gm = -4$, whereas Scenario II is represented as $Gr = 2$ and $Gm = 4$.

Variations of the penetrability parameter on speed are visualized graphically in Fig. 2. This figure indicates that velocity rises for Scenario II and decreases in velocity for Scenario I. The impact of the Eckert number appears in Fig. 3. Higher Ec leads to higher viscous dissipation, which increases the temperatures of the liquid, reduces resistance, and consequently results in higher speed. The Eckert number generally lies in the range of 0.01–2.0. Physically, a higher Eckert number indicates stronger viscous dissipation, which raises the fluid temperature. Fig. 4 displays the velocity graph against the permeability parameter. From Fig. 4, velocity increases when the flow is over a cooled plate (Scenario II) and decreases when the flow is over a heated plate (Scenario I). Fig. 5 presents the outline of velocity distribution for distinct estimations of the magnetic field, showing that velocity reduces in Scenario II and increases in Scenario I. The finding of Fig. 5 proves that the magnetic field will, in general, decelerate flow on the cooled plate, whereas the reverse effect occurs on the heated plate. The different effects on Scenario I and II can be described as caused by the obligation of the transverse magnetized force of strength B_0 in a liquid flow model, it creates in the electrically conducting fluid a resistive kind of power, noted as Lorentz power, which acts next to the comparative motion of the fluid. Physically, when a magnetic field is applied perpendicularly to the flow direction, and the fluid is conducting, electric currents are induced. Applying a transverse magnetic field to an electrically conducting fluid generates a Lorentz force. This force acts opposite to the direction of fluid motion, creating a resistive or braking effect that slows down the flow of a phenomenon known as magnetic damping. The magnetic parameter M typically ranges from 0 to 20. Fig. 6 displays the velocity graph versus Gr. This parameter indicates the influences of the buoyancy force (caused by temperature gradient) and the viscous force. These forces influence the increment in velocity by this pattern: The enhancement in buoyancy force and the decrement in viscous force, which directly increases Gr parameter. Fig. 7 displays a velocity graph for different Gm values, characterized by buoyancy force (due to mass gradient) and viscous force. As estimated, velocity enhances, and high value is distinctive because of buoyancy force increases on species. Fig. 8 depicts the response to velocity distributions for diverse values of S_0. This graph shows that the velocity significantly accelerates with the Soret number in Scenario II. However, the velocity is accelerated when the flow is on a heated plate (Scenario I). The influences of Kr on the speed outlines are explained in Fig. 9. The dimensionless velocity somewhat reduces with Kr, and the reverse happened in the other case. Fig. 10 indicates the impacts of Sc on the speed outline. It is discovered that if Sc reduces, the flow over a cooled plate slows down, whereas the fluid flow motion is accelerated over a heated plate. Fig. 11 represents the influences of an inclination of the surface. With the effect of rising inclination angle, the velocity increases when the region of the fluid is over a heated plate. However, the velocity decreases for the cooled plate with increasing inclination factor. The maximum velocity is reached when the plate is placed vertically. However, when the plate is projected at a certain angle, the effect of the buoyancy force is lessened because of the gravitational acceleration vector. The impact of Prandtl numbers Pr on the speed component is depicted in Fig. 12. It is remarked that the velocity is decreased when the fluid flows over a cooled plate, whereas

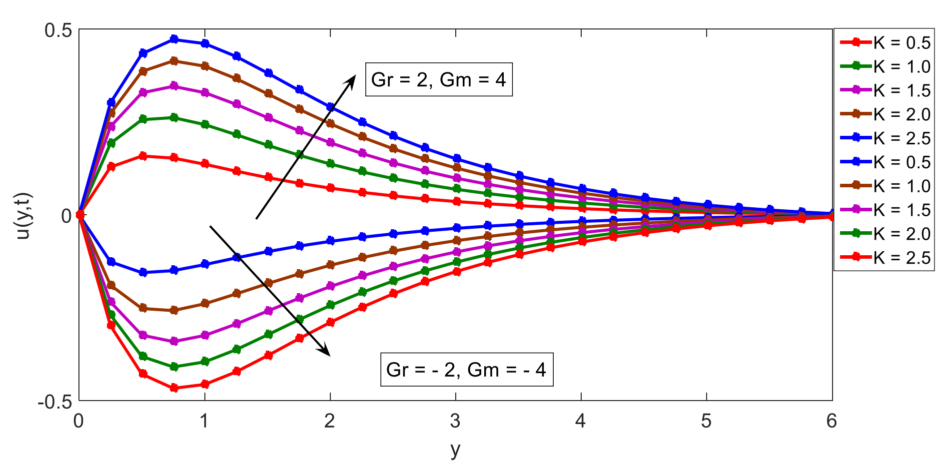

Fig. 2. The flow velocity versus K.

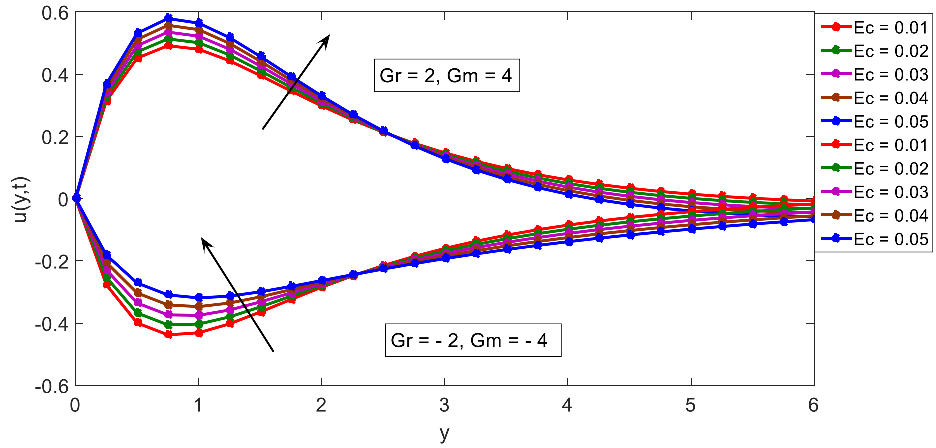

Fig. 3. The flow velocity versus *Ec*.

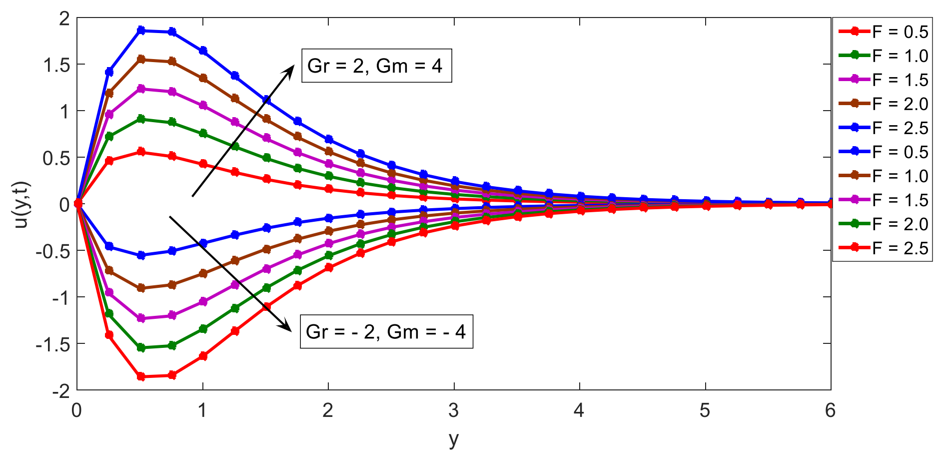

Fig. 4. The flow velocity versus *F*.

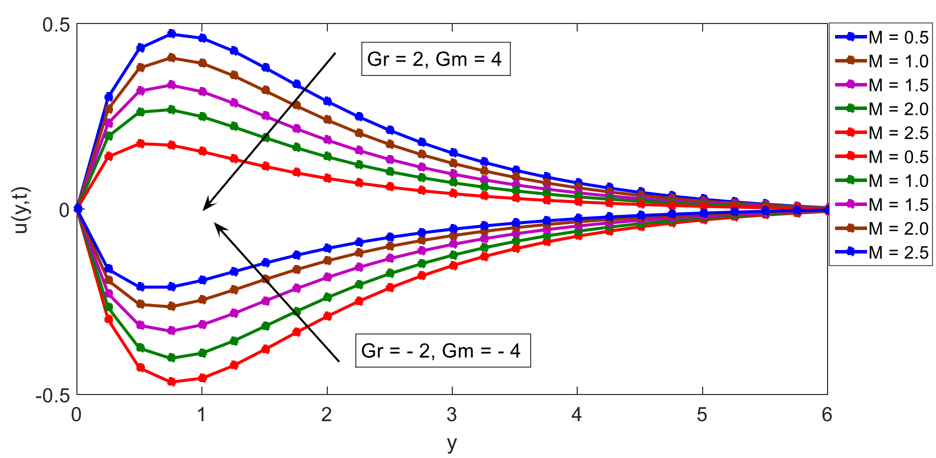

Fig. 5. The flow velocity versus *M*.

velocity produces an opposite pattern at a heated plate.

Fig. 13 establishes the dependence of the Prandtl numbers (Pr) on fluid temperatures. This graph shows that the temperature decreases when Pr increases. An increase in Pr corresponds to the lower thermal conductivity values. As a result, the temperature is decreased. This impact of the heat generating Q on the temperatures outline is comprehended in Fig. 14. It seems reasonable that when Q rises, it will fall. The heat source itself does not reduce temperature, but it can modify the system dynamics (like inducing stronger convection or triggering radiative loss), leading to a lower steady-state temperature in some regions. Fig. 15 shows that fluid temperatures fall when the thermal radiative parameter rises. Radiation reduces temperature by propagating energy away from the surface or fluid in the form of electromagnetic waves. This behavior occurs because thermal radiation acts as a heat loss mechanism. It transfers thermal energy away from the fluid and surface through electromagnetic waves. As radiation becomes more significant,

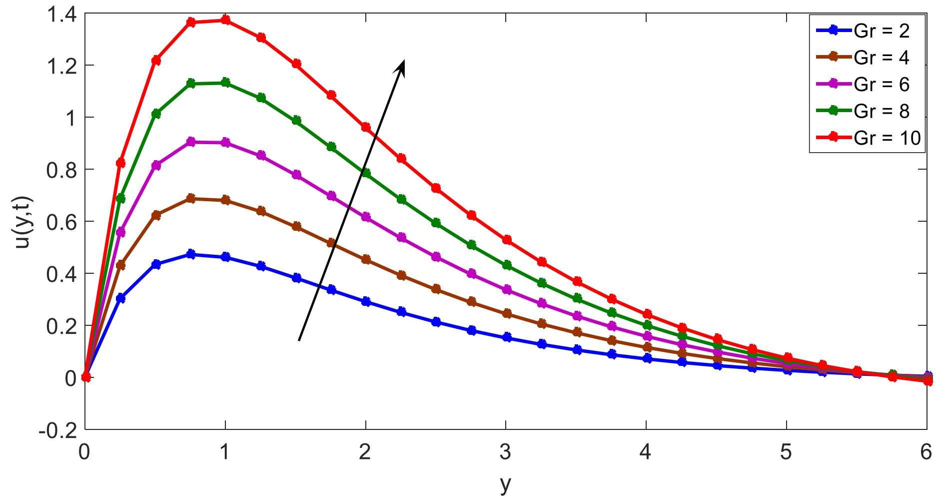

Fig. 6. The flow velocity versus *Gr*.

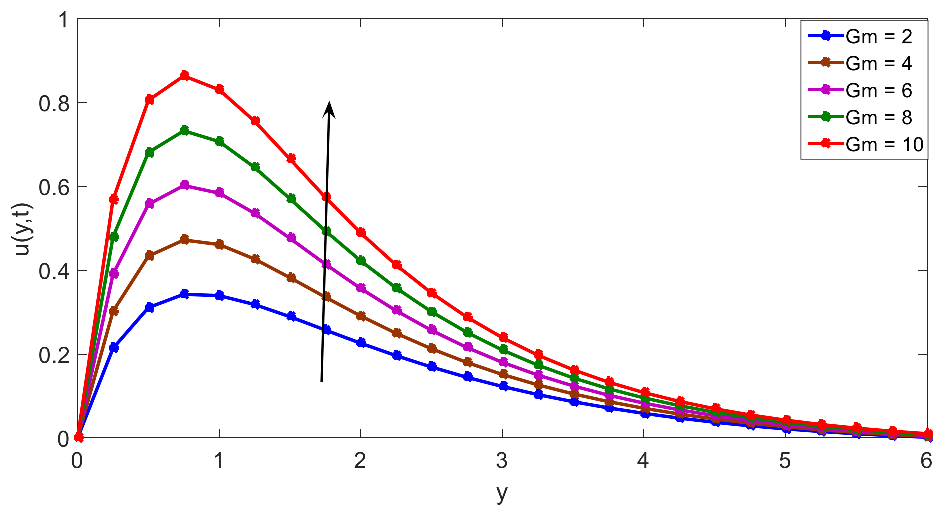

Fig. 7. The flow velocity versus *Gm*.

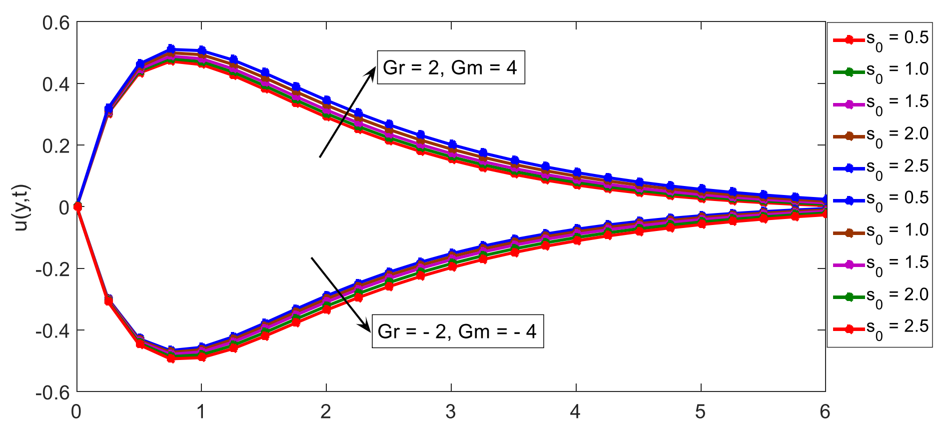

Fig. 8. The flow velocity versus S_0.

more heat is dissipated from the fluid to its surroundings. The consequences of the Soret numbers on the temperatures outline are illustrated in Fig. 16. As the parameter S_0 increased, and temperature patterns increased. The Soret number increases the temperature profile indirectly by enhancing species diffusion toward high-temperature regions, which may intensify chemical reactions or heat generation. Fig. 17 demonstrates the effects of *Ec* on the temperatures profile. An upsurge in Eckert numbers leads to higher temperatures outline caused by it enhances

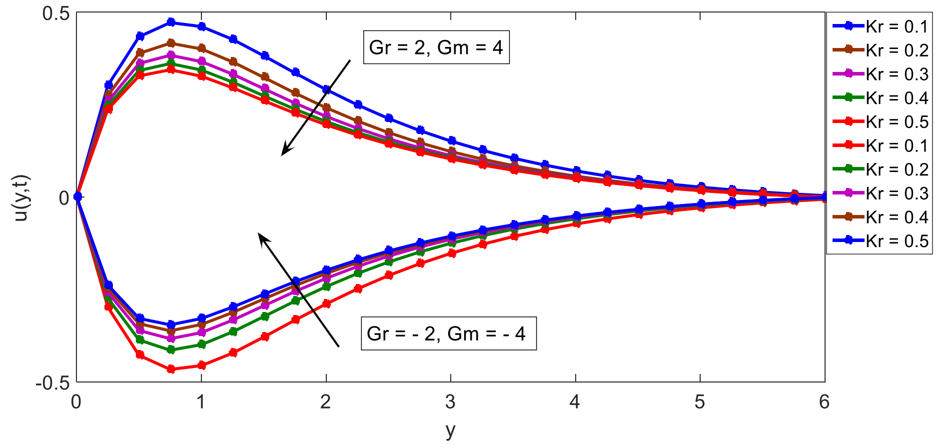

Fig. 9. The flow velocity versus *Kr*.

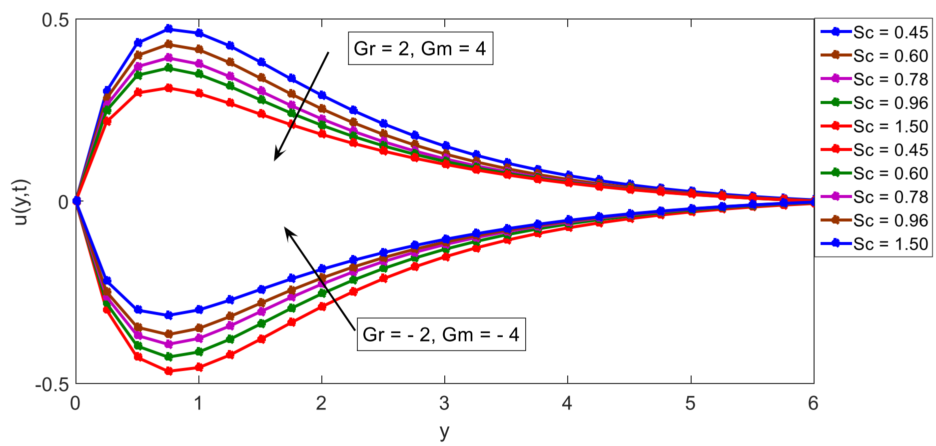

Fig. 10. The flow velocity versus *Sc*.

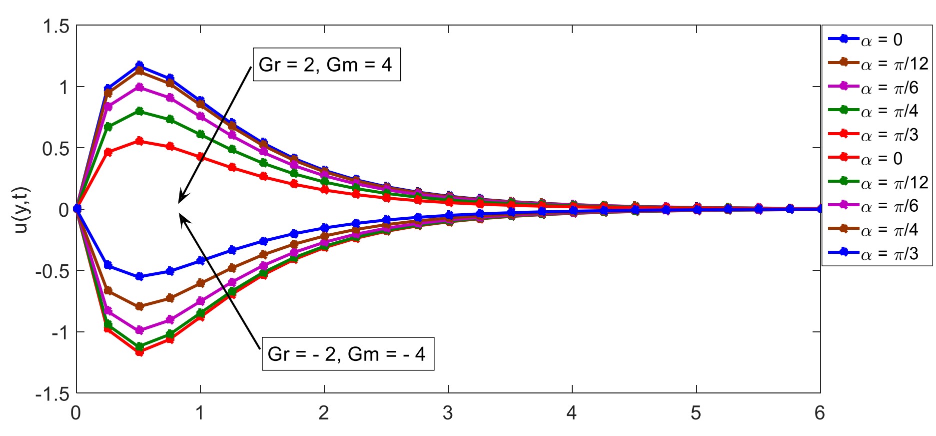

Fig. 11. The flow velocity versus α.

viscous dissipation, converting kinetic energy into heat within the flow.

Fig. 18 shows how a chemical reaction influences the concentration profile. This profile is decreased because of a chemically reactive process. A chemically reactive operation decreases the concentration of a species with the assumption that the species is a reactant. The concentration profile for varying Soret numbers is shown in Fig. 19. Here, when S_0 rises, the concentration also rises. The Soret effect causes mass diffusion driven by temperature gradients, leading to concentration enhancement. Fig. 20 illustrates the impact of species concentration for a range of Schmidt's numbers (*Sc*). It may be understood physically as the ratio between momentum and molecule diffusivities. A higher Schmidt number means slower mass diffusion, which can result in lower concentrations. Fig. 21 demonstrates the effects of Eckert numbers on the concentration profile. This parameter increases concentration indirectly by raising the temperature via viscous dissipation, which enhances thermodiffusion and reaction rates, leading to higher local species concentrations.

Fig. 22 displays the surface frictional factor concerning the Eckert

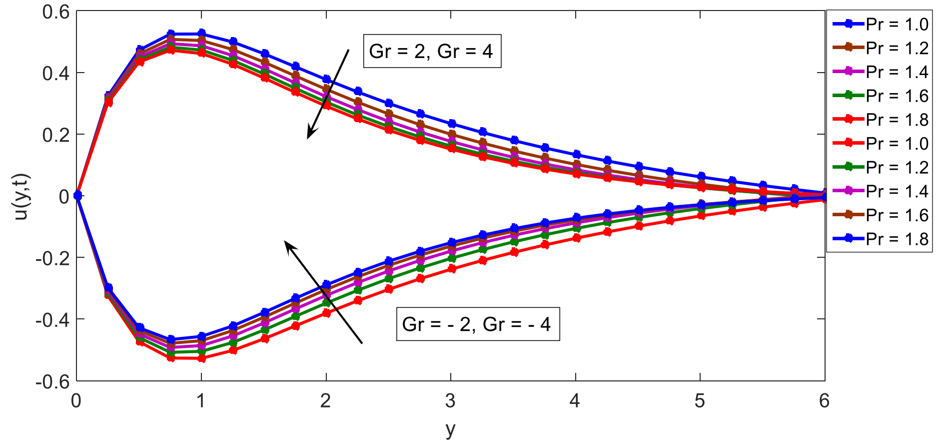

Fig. 12. The flow velocity versus *Pr*.

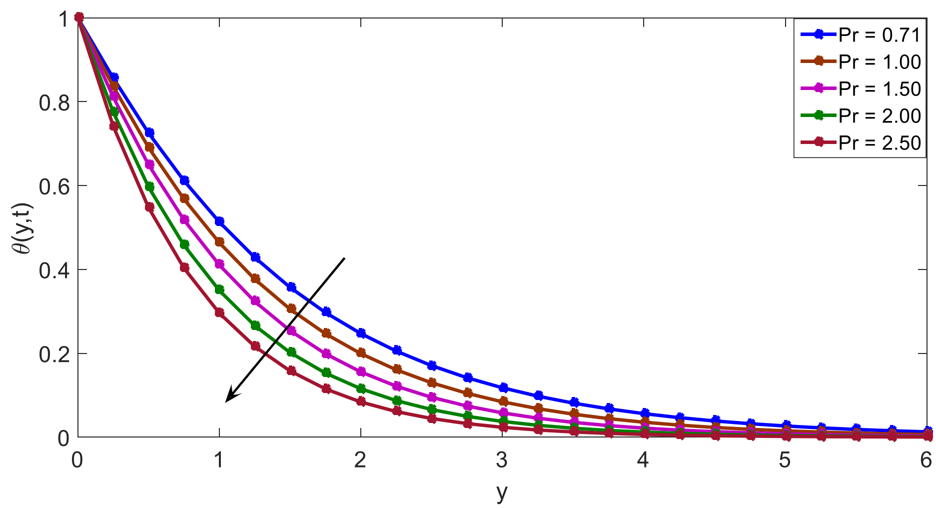

Fig. 13. The fluid temperatures versus *Pr*.

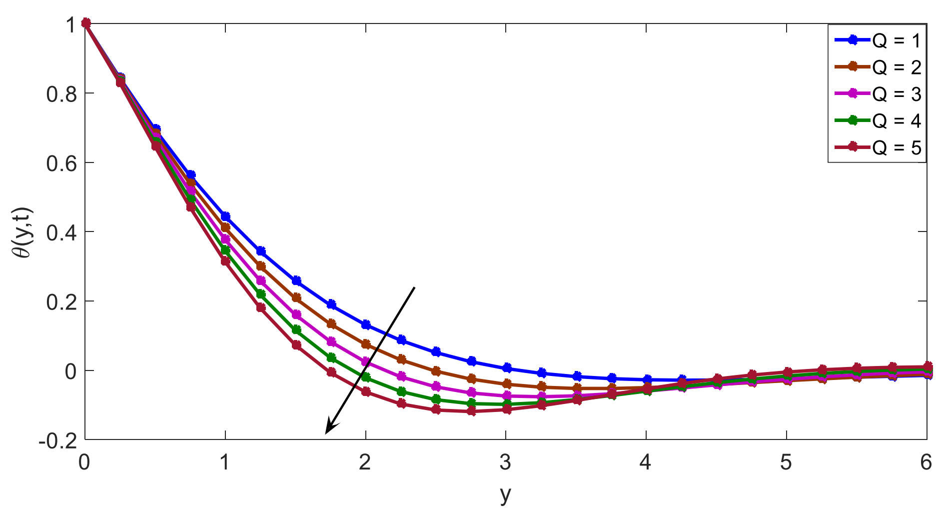

Fig. 14. The fluid temperatures versus *Q*.

numbers for various Grashof number values, showing that the impact of *Gr* reduces the surface frictional factor. An increment in the Grashof number diminishes the surface frictional factor by enhancing buoyancy-driven flow, which weakens the wall shear stress. The relationship between Nusselt number and heat-generating variable *Q* is revealed in Fig. 23. It has been shown that rising heat production leads to an upsurge in the Nusselt numbers. Fig. 24 depicts the relationship between the Nusselt and Eckert numbers as a function of the radiation parameter

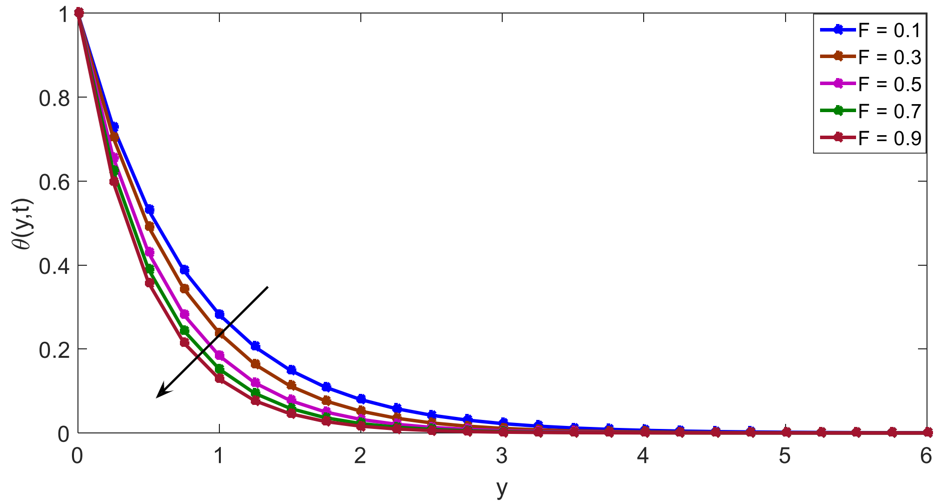

Fig. 15. The fluid temperatures versus F.

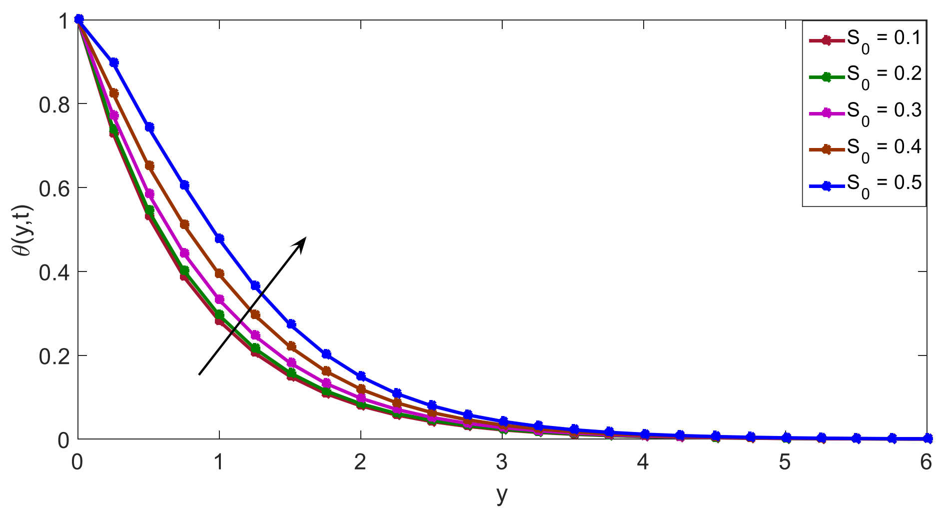

Fig. 16. The fluid temperatures versus S_0.

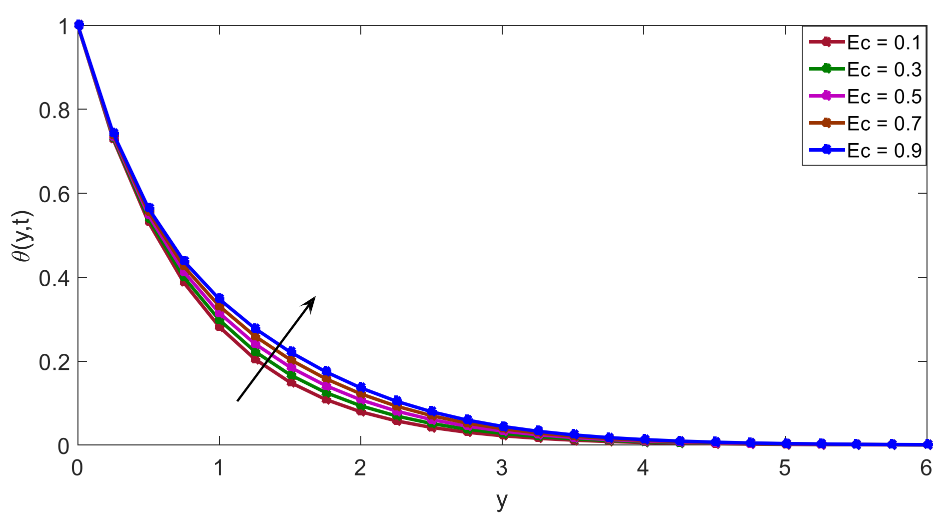

Fig. 17. The fluid temperatures versus Ec.

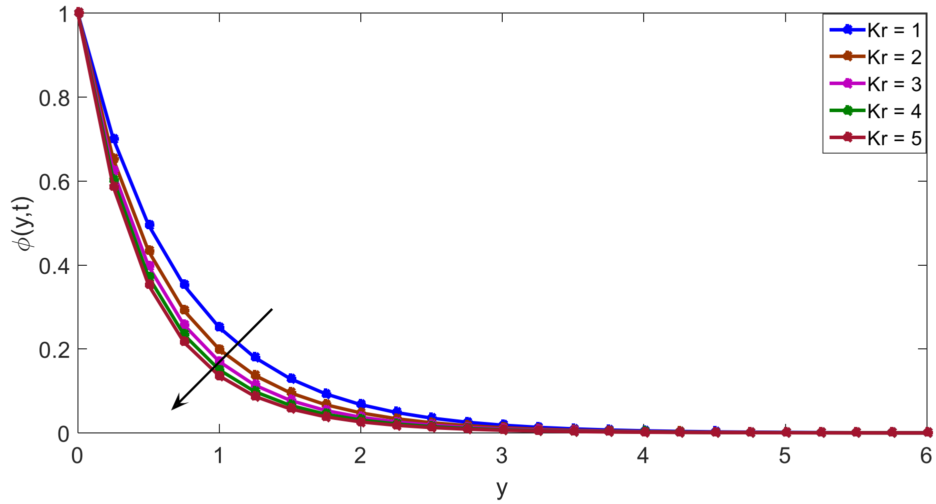

Fig. 18. The fluid concentrations versus *Kr*.

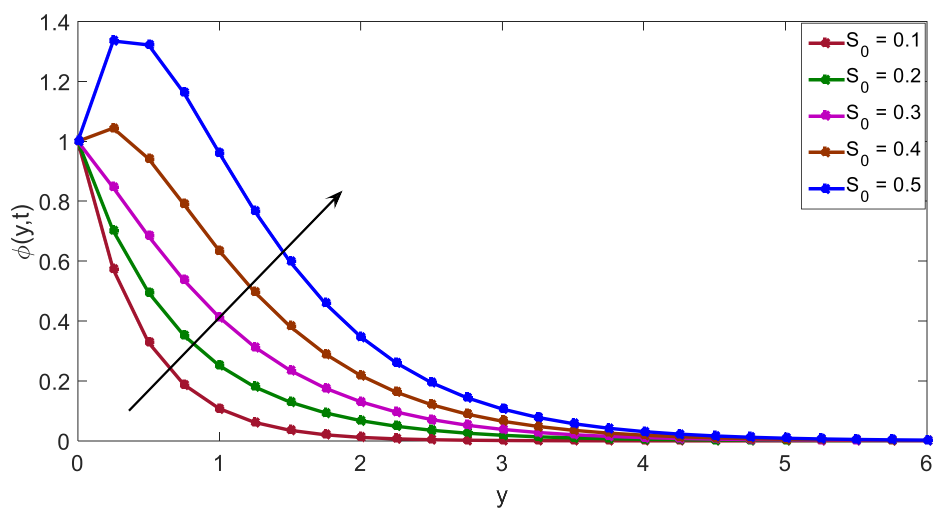

Fig. 19. The fluid concentrations versus S_0.

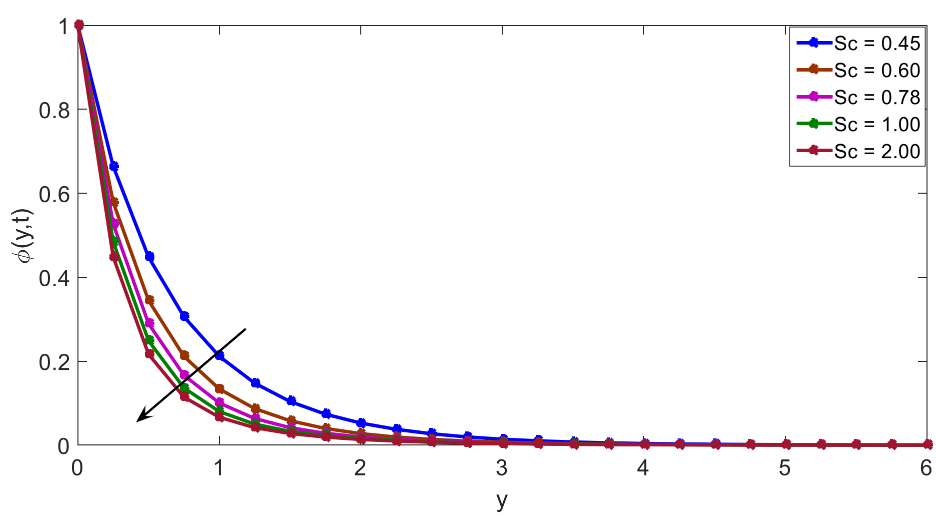

Fig. 20. The fluid concentrations versus *Sc*.

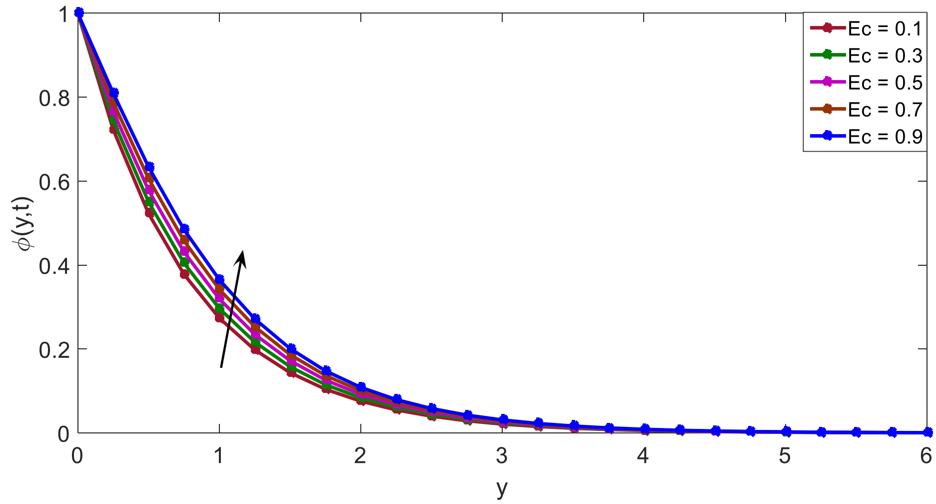

Fig. 21. The fluid concentrations versus *Ec*.

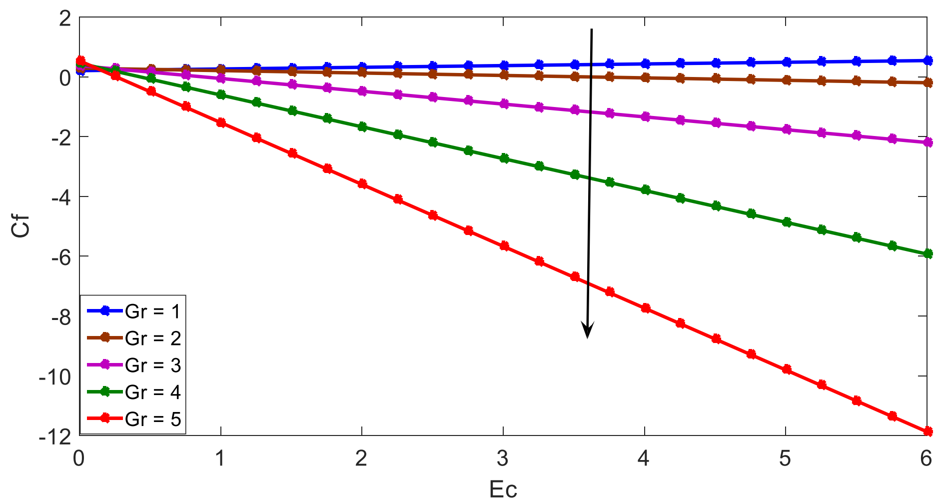

Fig. 22. Impacts of *Gr* on wall frictional factor.

F. As *F* rises, the Nusselt number is shown to fall. Figs. 25 and 26 show the relationship between the Sherwood and Eckert numbers as a function of the Schmidt and Soret numbers, respectively. Sherwood's number goes down as Schmidt's and Soret's do, and vice versa.

5. Conclusions

Radiation effects on an infinitely sloped plate have been solved analytically, considering viscous dissipation and Joule heating.

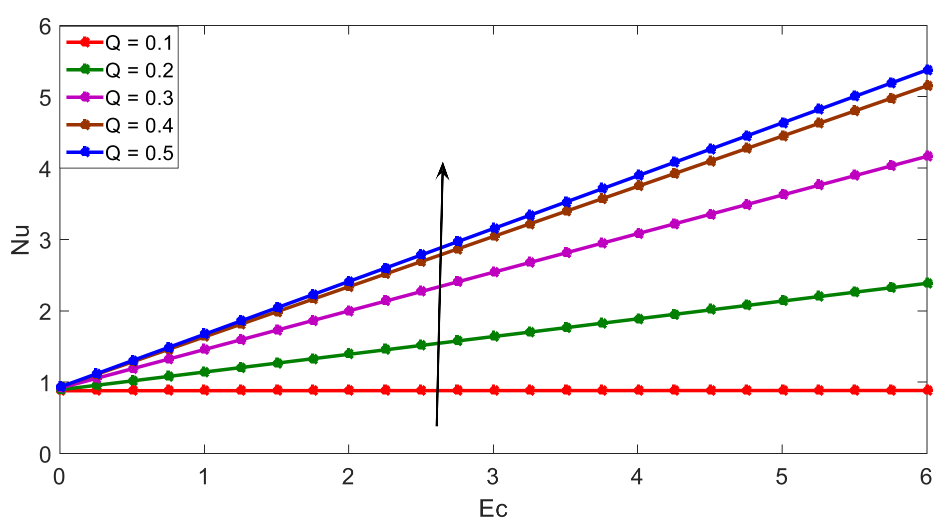

Fig. 23. Impacts of *Q* on Nusselt numbers.

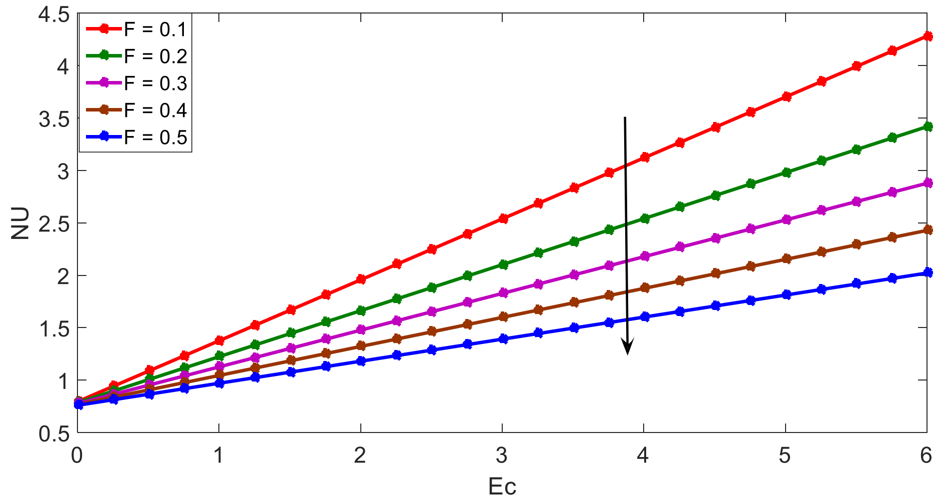

Fig. 24. Impacts of F on Nusselt numbers.

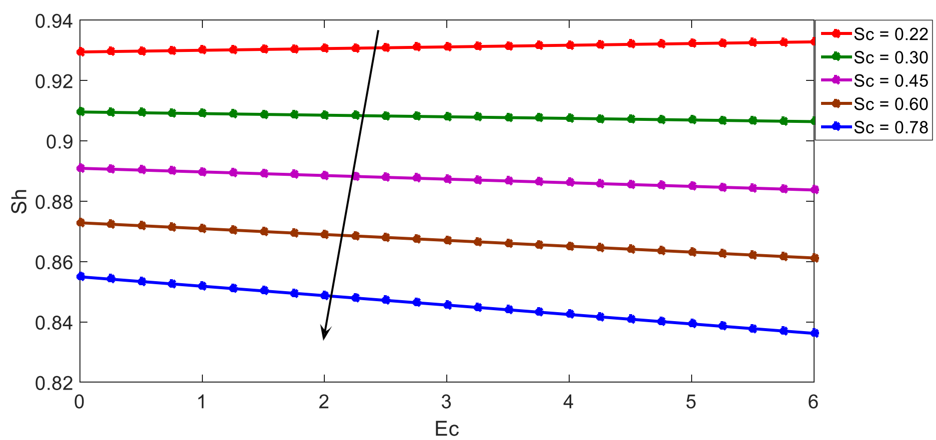

Fig. 25. Impacts of Sc on Sherwood numbers.

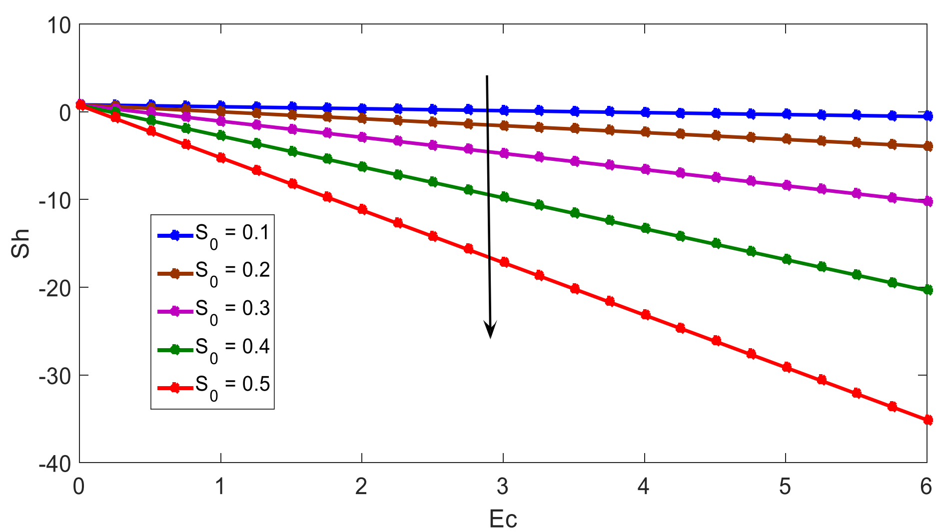

Fig. 26. Impacts of S_0 on the Sherwood numbers.

MATLAB was used to solve the dimensionless governing equations for diverse factors like the mass Grashof and the thermal Grashof numbers, the Prandtl number, thermal radiative flux, heat source, the Soret number, and the Schmidt number. Graphical representations of surface frictional factors, Nusselt numbers, Sherwood numbers, velocity, temperature, and concentrations, along with the influences of diverse variables. The following findings emerged from the solutions mentioned above and the outcomes and discussions. Non-dimensional factors positively impact velocities, surface frictional factors, dimensionless temperatures, heat and mass transfer rates, and concentrations:

- The velocity is accelerated due to the impact of the mass Grashof and thermal Grashof numbers.
- Temperature declines caused the increasing Prandtl numbers.
- The impacts of thermal radiative flux on temperatures and Nusselt numbers are significant because it reduces the temperature and Nusselt number.
- The temperatures are reduced, and the Nusselt numbers are enhanced by the same parameter, which is the heat-generating variable.
- The temperatures and concentrations are enhanced by the Soret number. However, this parameter reduces the Sherwood numbers.
- The Schmidt numbers reduce the concentrations and the Sherwood numbers.

Funding

This research work was funded by Umm Al-Qura University, Saudi Arabia under grant number: 25UQU4240148GSSR02.

CRediT authorship contribution statement

Syed M. Hussain: Investigation. **Hina Zahir:** Writing – original draft. **Muhamamd Taskeen Raza:** Methodology. **Bandar M. Fadhl:** Software. **Mohamed R. Eid:** Validation, Resources, Writing – review & editing. **Wasim Jamshed:** Writing – original draft, Methodology. **Siti Suzilliana Putri Mohamed Isa:** Resources, Data curation, Conceptualization. **Kamel Guedri:** Supervision, Project administration, Investigation.

Conflicts of interest

There is no conflict of interest.

Acknowledgments

The authors extend their appreciation to Umm Al-Qura University, Saudi Arabia for funding this research work through grant number: 25UQU4240148GSSR02.

Nomenclature

B_0	Magnetic field strength (A/m)
Ec	Eckert number ($-$)
F	Radiation parameter
Gr	Thermal Grashof number
Gm	Mass Grashof number
Nu	Nusselt numbers
Sh	Sherwood numbers
u^*, v^*	Velocity elements in the x^* and y^* orientations (m/s)
C_w	Concentration near the surface (mol/m^3)
C_p	Fluid specific heat at a fixed pressure ($J/kg.K$)
M	Hartmann number
Kr	Chemical reaction parameter
S_0	Soret number
D	Mass diffusivity (m^2/s)
D_1	Coefficient of thermal diffusivity (m^2/s)
ν_0	Constant suction velocity (m/s)
k	Fluid thermal conductance ($W/m.K$)
m	Hall current parameter
K^*	The permeability of the porous material (m^2)
g	Acceleration due to gravity (m/s^2)
T^*	Temperature of the fluid (K)
T_w	Temperature near the plate (K)
T_∞	Temperature far away from the surface (K)
Pr	Prandtl number
C^*	Concentration of the fluid (mol/m^3)
C_∞	Concentration far away from the plate (mol/m^3)
Sc	Schmidt number
Q	Heat generation parameter
Greek Symbols	
ϕ	Dimensionless concentration
β	Thermal expansion coefficient ($1/K$)
σ	Magnetic permeability of the fluid (S/m)
ρ	Density (kg/m^3)
τ	Wall frictional factor (N/m^3)
α	Inclination angle (degree)
θ	Nonimensional temperatures
υ	Fluid kinematic viscosity (m^2/s)
β^*	Mass expansion coefficient (m^3/kg)
μ	Dynamic viscosity ($Pa.s$)
$'$	Superscript belongs to differentiations concerning y

References

Alam, M. S., Rahman, M. M., & Sattar, M. A. (2008). Effects of variable suction and thermophoresis on steady MHD combined free-forced convective heat and mass transfer flow over a semi-infinite permeable inclined plate in the presence of thermal radiation. *International Journal of Thermal Sciences, 47*, 758–765.

Alam, M. S., Rahman, M. M., & Sattar, M. A. (2009). On the effectiveness of viscous dissipation and Joule heating on steady Magnetohydrodynamic heat and mass transfer flow over an inclined radiate isothermal permeable surface in the presence of thermophoresis. *Communications in Nonlinear Science and Numerical Simulation, 14*, 2132–2143.

Ananda Reddy, N., Varma, S. V. K., & Raju, M. C. (2009). Thermo diffusion and chemical effects with simultaneous thermal and mass diffusion in MHD mixed convection flow with Ohmic heating. *Journal of Naval Architecture and Marine Engineering, 6*, 84–93.

Cess, R. D. (1966). The interaction of thermal radiation with free convection heat transfer. *International Journal of Heat and Mass Transfer, 9*, 1269–1277.

Chien-Hsin, C. (2004). Combined heat and mass transfer in MHD free convection from a vertical surface with Ohmic heating and viscous dissipation. *International Journal of Engineering Science*, (42), 699–713.

Das, S. S., Sahoo, S. K., & Dash, G. C. (2006). Numerical solution of mass transfer effects on unsteady flow past an accelerated vertical porous plate with suction. *Bull. Malays. Math. Sci. Soc., 29*(1), 33–42.

Das, S. S., Tripathy, U. K., & Das, J. K. (2010). Hydromagnetic convective flow past a vertical porous plate through a porous medium with suction and heat source. *International Journal of Energy and Environment, 1*(3), 467–478.

Dharmaiah, G., Chamkha, Ali. J., Vedavathi, N., & Balamurugan, K. S. (2019). Viscous dissipation effect on transient aligned magnetic free convective flow past and inclined moving plate. *Frontiers in Heat and Mass Transfer (FHMT), 12*(17), 1–11. ISSN: 2151-8629.

Dharmaiah, G., Makinde, O. D., & Balamurugan, K. S. (2020). Perturbation analysis of thermophoresis, hall current and heat source on flow dissipative aligned convective flow about an inclined plate. *International Journal of Thermofluid Science and Technology, 7*(1), Article 20070103. Paper No.

Dharmaiah, G., Sridhar, W., Farhany, K. A. L., Balamurugan, K. S., & Ali, F. (2022). Non-Newtonian nanofluid characteristics over a melting wedge: A numerical study. *Heat Transfer, 51*(5), 4620–4640.

Eid, M. R., & Mishra, S. (2017). Exothermically reacting of non-Newtonian fluid flow over a permeable nonlinear stretching vertical surface with heat and mass fluxes. *Computational Thermal Sciences: International Journal, 9*(4), 283–296.

Eswaramoorthi, S., Nasir, S., Loganathan, K., Gupta, M. S., & Berrouk, A. (2025). Numerical simulation of rotating flow of CNT nanofluids with thermal radiation, ohmic heating, and autocatalytic chemical reactions. *Alexandria Engineering Journal, 113*, 535–550.

Eswaramoorthi, S., & Sivasankaran, S. (2022). Entropy optimization of MHD Casson-Williamson fluid flow over a convectively heated stretchy sheet with Cattaneo-Christov dual flux. *Scientia Iranica, 29*(5), 2317–2331.

Ganesan, P., Suganthi, R. K., & Loganathan, P. (2013). Viscous and ohmic heating effects in doubly stratified free convective flow over vertical plate with radiation and chemical reaction. *Appl. Math. Mech. Engl. Ed., 34*(2), 139–152.

Gebhart, B. (1962). Effect of viscous dissipation in natural convection. *Journal of Fluid Mechanics, 14*(2), 225–232.

Ibrahim, S. Y., & Makinde, O. D. (2010). Chemically reacting MHD boundary layer flow of heat and mass transfer over a moving vertical plate with suction. *Scientific Research and Essays, 5*(19), 2875–2882.

Isa, S. S. P. M., Som, A. N. M., & Balakrishnan, N. (2024). Heat/mass transfer performance in magnetohydrodynamics Carreau hybrid nanofluid with dual nanoparticles (molybdenum disulfide and silica). *Magnetohydrodynamics*, (0024-998X), 60.

Karraiah, A. S., Kesaraiah, D., & Bhavana, M. (2013). The Soret effect on free convective unsteady MHD flow over a vertical plate with heat source. *International Journal of Innovative Research in Science, Engineering and Technology, 2*(5), 1617–1628.

Kumar, T. P., Dharmaiah, G., Al-Farhany, K., Alomari, M. A., Flayyih, M. A., Jamshed, W., & Isa, S. S. P. M. (2023). Perturbation methodology for electromagnetic radiative fluxing of chemical reactive Casson fluid flow under heat source (sink) effectiveness. *International Journal of Modern Physics B, 37*(28), Article 2350243.

Makinde, O. D. (2005). Free convection flow with thermal radiation and mass transfer past a moving vertical porous plate. *International Communications in Heat and Mass Transfer, 32*, 1411–1419.

Makinde, O. D. (2012). Chemically reacting hydromagnetic unsteady flow of a radiating fluid past a vertical plate with constant heat flux. *Zeitschrift für Naturforschung, 67*, 239–247.

Makinde, O. D., & Mhone, P. Y. (2005). Heat transfer to MHD oscillatory flow in a channel filled with porous medium. *Romanian Journal of Physics, 50*(9–10), 931–938.

Makinde, O. D., & Olanrewaju, P. O. (2010). Buoyancy effects on thermal boundary layer over a vertical plate with a convective surface boundary condition. *Transactions ASME Journal of Fluids Engineering, 132*(1–4), Article 044502.

Mallawi, F. O. M., Eswaramoorthi, S., Sivasankaran, S., & Bhuvaneswari, M. (2022). Impact of stratifications and chemical reaction on convection of a non-Newtonian fluid in a Riga plate with thermal radiation and Cattaneo-Christov flux. *Journal of Thermal Analysis and Calorimetry, 147*(Issue 11), 6519–6535.

Nandkeolyar, R., Seth, G. S., Makinde, O. D., Sibanda, P., & Ansari, M. S. (2013). Unsteady hydromagnetic natural convection flow of a dusty fluid past an impulsively moving vertical plate with ramped temperature in the presence of thermal radiation. *ASME J. Appl. Mech., 80*(6), Article 061003.

Osalusi, E., Side, J., Harris, R., & Johnston, B. (2007). On the effectiveness of viscous dissipation and Joule heating on steady MHD flow and heat transfer of a Bingham fluid over a porous rotating disk in the presence of Hall and ion-slip currents. *International Communications in Heat and Mass Transfer, 34*, 1030–1040.

Prasad, T. V., Linga Raju, T., & Rajakumar, K. V. B. (2023). Viscous dissipation and radiation absorption effects on unsteady MHD free convective fluid flow past an inclined porous plate with chemical reaction. *Heat Transfer, 52*(2), 1254–1274. https://doi.org/10.1002/htj.22739

Rahman, A. T. M. M., Alam, M. S., & Chowdhury, M. K. (2012). Local similarity solutions for unsteady two-dimensional forced convective heat and mass transfer flow along a wedge with thermophoresis. *International Journal of Applied Mathematics and Mechanics, 8*(8), 86-11.

Rajakumar Komaravolu, V. B., Rao, T. G., Balamurugan, K. S., & Rani, C. B. (2025). Cross diffusion effects on magnetohydrodynamic free convective flow over a vertical porous plate under the influence of chemical reactions. *Thermal Radiation, and Dissipative Heating. Heat Transfer*.

Rajakumar, K. V., Pavan Kumar Rayaprolu, V. S., Balamurugan, K. S., & Kumar, V. B. (2020). Unsteady MHD Casson dissipative fluid flow past a semi-infinite vertical porous plate with radiation absorption and chemical reaction in presence of heat generation. *Mathematical Modelling of Engineering Problems, 7*(1). https://doi.org/10.18280/mmep.070120

Rajakumar, K. V. B., Ranganath, N., Govinda Rao, T., & Srinivasa Raju, R. (2024a). Radiation absorption, Hall and ion-slip current–driven MHD convection with spanwise cosinusoidally fluctuating temperature: A perturbative study. *Radiation Effects and Defects in Solids*, 1–35. https://doi.org/10.1080/10420150.2024.2391775

Rajakumar, K. V. B., Sreenivasulu, G., & Balamurugan, K. S. (2024b). Influence of heat flow due to concentration gradient on unsteady MHD heat and mass transform dissipative flow with spanwise fluctuating temperature. *Numerical Heat Transfer, Part A: Applications*, 1–26.

Rashidi, M. M., & Erfani, E. (2012). Analytical method for solving steady MHD convective and slip flow due to a rotating disk with viscous dissipation and Ohmic heating. *Eng.Computation, 29*(6), 562–579.

Reddy, V. S., Kandasamy, J., & Sivanandam, S. (2023). Stefan blowing impacts on hybrid nanofluid flow over a moving thin needle with thermal radiation and MHD. *Computation, 11*(7), 128. https://doi.org/10.3390/computation11070128

Sandeep and Sugunamma. (2013). Aligned magnetic field and chemical reaction effects on flow past a vertical oscillating plate through porous medium. *Communications in Applied Sciences, 1*(Number 1), 81–105, 2013.

Sindhu, R., Alessa, N., Eswaramoorthi, S., & Loganathan, K. (2023). Comparative analysis of Darcy–Forchheimer radiative flow of a water-based Al_2O_3-Ag/TiO_2 hybrid nanofluid over a Riga plate with heat sink/source. *Symmetry, 15*(Issue 1), 199. https://doi.org/10.3390/sym15010199

Srinivasa Reddy, V., Kandasamy, J., & Sivanandam, S. (2024). Joule heating, Dufour and Soret effects on MHD hybrid nanoliquid flow over a moving thin needle in a porous medium with thermal radiation. *World Journal of Engineering*. https://doi.org/10.1108/WJE-01-2024-0040

Zhou, X., Qureshi, M. A., Khan, N., Jamshed, W., Isa, S. S. P. M., Balakrishnan, N., & Hussain, S. M. (2024). Thermosolutal Marangoni convective flow of MHD tangent hyperbolic hybrid nanofluids with elastic deformation and heat source. *Open Physics, 22*(1), Article 20240082.